Available online at www.sciencedirect.com
SciVerse ScienceDirect
Procedia CIRP 6 (2013) 238 – 243

www.elsevier.com/locate/procedia

The Seventeenth CIRP Conference on Electro Physical and Chemical Machining (ISEM)

Influence of workpiece circumferential speed in wire electrical discharge machining

E. Weingärtner[a]*, K. Wegener[a], F. Kuster[a]

[a]Institute of Machine Tools and Manufacturing, ETH, Tannenstrasse 3, Zurich 8092, Switzerland
* Corresponding author. Tel.: +41-43-632-0495; fax: +41-44-632-1125. *E-mail address*: weingaertner@iwf.mavt.ethz.ch.

Abstract

In Wire Electrical Discharge Machining (WEDM) a specific wire run-off speed is applied to compensate wear and avoid wire breakage. Since the workpiece generally stays stationary and short discharge durations are applied, the relative displacement between wire and workpiece during one single discharge is very small. In Wire Electrical Discharge Dressing (WEDD), however, the workpiece rotates at very high circumferential speeds, since dressing is usually performed at grinding speeds. In this work the influence of relative speed in WEDM is assessed. Single discharge experiments were first carried out using circumferential speeds up to 80 m/s. The plasma channel was found to easily slide over the anode, creating elongated craters, and higher removal per single discharge was measured for higher relative speeds. A thermo-electrical model was used to help understand the process, showing that higher melting efficiencies can be reach as relative speeds are increased. The model was also used to predict damages to diamonds grains used in metal bonded grinding wheels. It was found that even if the plasma channel slides over a diamond due to the relative speed, graphitization is not likely to occur.

Keywords: Dressing; Diamond; Wire EDM; Thermo-electrical model.

1. Introduction

In electrical discharge machining low relative speeds between tool electrode and workpiece are usually applied. In sinking EDM, electrode tool rotation is in most cases not applicable, since complex workpiece geometries are created using shaped electrodes. In EDM drilling and milling, however, tool rotation can be used, which helps improve flushing and therefore positively impacts material removal rates [1]. Yet, relative speed is still very low in these cases, since small electrode diameters are commonly used. In wire EDM, the workpiece stays stationary in most of the cases while the wire is fed from a spool with run-off speeds ranging from around 2 to 20 m/min. Axisymmetric workpieces can also be machined by means of WEDM, in which a rotary axis is added to the EDM machine, such as in cylindrical wire electrical discharge turning (CWEDT) [2-4]. Wire electrical discharge grinding (WEDG) also deals with rotating workpieces [5, 6]. In both processes, however, relatively low rotation speeds are applied. On the other hand, high relative speeds are used in on-machine electrical discharge dressing [7, 8], since the grinding wheel, in general, has to be conditioned using the same rotating speed as for grinding, to avoid errors caused by centrifugal forces. Thus, in EDD relative speeds around 100 m/s can be used, what can impact the erosion process. If 100 m/s is used and a discharge duration of 2 µs is applied, the relative displacement during a single discharge would equal to 200 µm, which in most cases is larger than the size of eroded craters.

The influence of relative speeds during EDM is still not yet fully understood. While some authors [2, 3, 9] indicate that the relative speed negatively impact material removal rates, some others [10, 11] describe the opposite, pointing out that the material removal rate can be increased as relative speeds are increased. Uhlman et al. [12] pointed out that small eroded craters were created by increasing speeds above 2.5 m/s while

doi:10.1016/j.procir.2013.03.063

Kunieda et al. [11] reported that elongated craters were created on the cathode while almost stationary discharge spots were observed on the anode.

In this work the influence of the relative speed in WEDM is assessed. Single discharge experiments were carried out for speeds up to 80 m/s and a thermo-electrical model was used to simulate single discharges.

2. Single discharge experiments

In this section the experimental setup used to perform single discharge experiments is first presented and experimental results are then discussed.

2.1. Experimental setup and results

To evaluate the influence of the relative speed on eroded craters, single discharge experiments were carried out using a self-designed wire electrical discharge dressing (WEDD) device, which was integrated inside a grinding machine (Fig. 01).

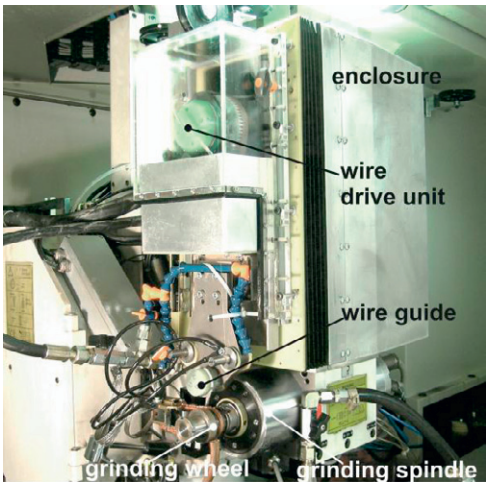

Fig. 01. WEDD-device used to perform single discharge experiments

This WEDD device is basically composed of a wire drive unit and a two axes feed system. The wire electrode is guided near to the erosion zone by means of a special wire guide system and can be moved in radial and axial directions relative to the grinding wheel. Single discharge experiments were performed using this device for relative speeds up to 80 m/s. The pulse interval time was set to be as long as possible, approximately 400 µs, so that consecutive discharges were eroded away from each other. Thus several craters were generated on the surface of the workpiece and could be measured separately.

Fig. 02 shows three craters eroded on a brass workpiece (CuZn39Pb3 - anode) using relative speeds of 0.5, 30 and 80 m/s, peak current of I_{peak} = 73 A and discharge duration t_e of 1.25 µs. It can be seen that the relative speed significantly influences the shape of eroded craters. The plasma slips over the anode and creates elongated craters in the relative speed direction.

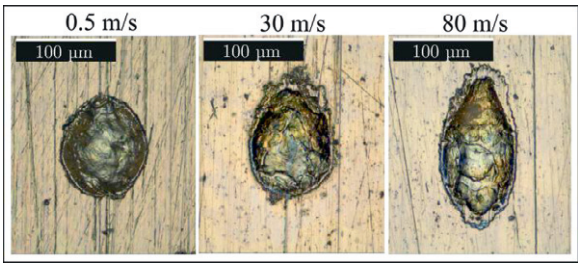

Fig. 02. Single discharge experiments by applying a peak current of 73 A and, discharge duration of 1.25 µs and different relative speeds

The relative speed applied during WEDM was found to influence not only the shape of the eroded craters as presented in Fig. 02 but also the amount of eroded volume per crater. An increase in the relative speed was found to cause an increase in the amount of eroded material. Results obtained by applying discharge peak currents of 73 and 157 A are presented in Fig. 03. When a peak current of I_{peak} = 73 A was applied, the eroded volume per crater rose from approximately 10,000 µm^3 to 20,000 µm^3 by rising the relative speed from v_r = 0.5 m/s to 80 m/s, while for I_{peak} = 157 A, it varied between around 35,000 µm^3 and 45,000 µm^3 for the same range of relative speeds.

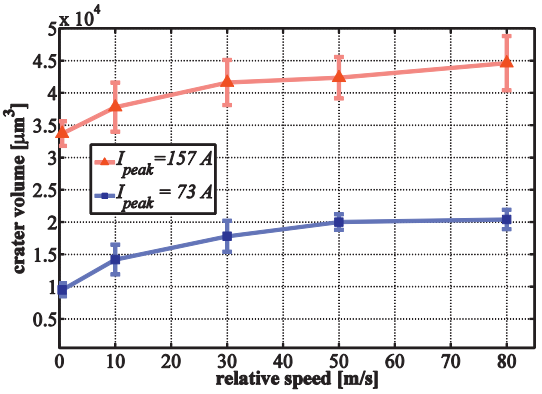

Fig. 03. Influence of the relative speed on eroded volume per crater for two different pulses (I_{peak} = 73 and 157 A; t_e = 1.25 and 1.35 µs)

The way how the size of eroded craters increases during the discharge can be assessed based on its shapes when high relative speeds are used, as shown in Fig. 02 for a relative speed of 80 m/s. It was found that the crater radius increases almost linearly until it reaches approximately 65% of the discharge duration and is kept nearly constant until the end of the discharge pulse. Fig. 04 shows a schematic representation of the crater radius

expansion as a function of discharge duration for an arbitrary discharge pulse, where the points a, b and c represent respectively the start location of the discharge, the position where it reaches its maximal radius and the center point of the crater at the end of the discharge. In these experiments electric current was delivered via capacitors (WEDM), i.e. the current peaks after approximately half of the discharge duration, and decreases continuously until the end of the discharge.

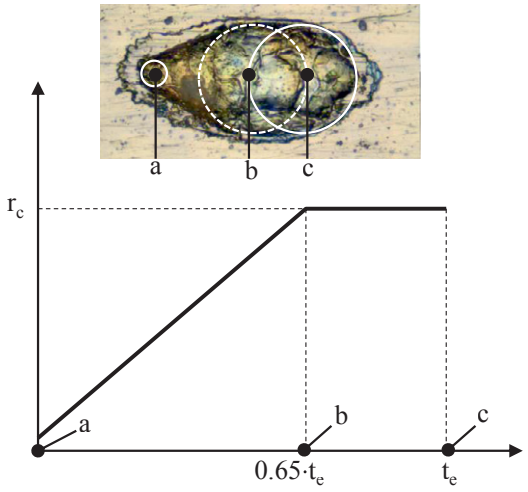

Fig. 04. Crater radius increase as a function of an arbitrary discharge duration: a) start point of discharge; b) point where crater reaches its maximum; c) center point of crater at the end of the discharge

To model the EDM process, it is important to know the way how the crater increases during the discharge, since better simulation results are achieved when a time-dependent heat source is considered, rather than a point heat source or a disc heat source. An empirical equation was thus derived to describe the crater radius expansion based only on the discharge duration t_e and peak current I_{peak}, which is used later in this work as input for an erosion model. Equation (1) describes approximately the curve presented in Fig. 04, where r_c increases almost linearly from point a to point b, and stays constant until it reaches point c. Table 1 shows results of measured crater radius obtained in single discharge experiments using six different types of discharge pulses, which were used as reference for Equation (1). Using I_{peak} in amperes and t_e in microseconds, the following solution was found: $a_0 = 27.84$; $a_1 = 0.225$; $a_2 = -0.00025$; $b_0 = -1.188$; $b_1 = 2.061$; $b_2 = 0.125$. The first part of the equation (coefficients a_n) describes the maximal crater size while the second part (coefficients b_n) describe the shape of the curve presented in Fig. 04, where the time t varies from 0 to t_e. It can be seen that the coefficient b_0 differs from zero, since we assumed a small plasma diameter at the beginning of the discharge to avoid almost infinite current density at this point.

$$r_c = \left(a_2 \cdot (i_{peak} \cdot t_e)^2 + a_1 \cdot (i_{peak} \cdot t_e) + a_0\right) \cdot \left(\left(\frac{b_2}{t_e^2}\right) \cdot t^2 + \left(\frac{b_1}{t_e}\right) \cdot t + b_0\right) \quad (1)$$

Table 1. Radius of eroded craters for different discharge pulses

Erosion pulses	I1	I2	I3	I4	I5	I6
Discharge duration, t_e [µs]	1.25	1.27	1.30	1.35	1.45	1.55
Discharge peak current, I_{peak} [A]	73	84	124	157	223	276
Eroded crater radius r_c [µm]	46.9	49.3	58.6	63.3	72.7	84.4

3. Modeling and simulation of WEDM

The WEDM model used in this work is based on the heat conduction phenomenon, assuming that heat generated in the plasma is transmitted to the workpiece via a specific heat source (in this case, neither a point heat source nor a disc heat source, but a time-dependent source, which grows from a point to a disc during the discharge duration). The partial differential equation that describes heat conduction in Cartesian coordinates is presented in Equation (2), and the thermal diffusivity α is described in Equation (3).

$$\frac{\partial^2 T}{\partial x^2} + \frac{\partial^2 T}{\partial y^2} + \frac{\partial^2 T}{\partial z^2} + \frac{\dot{q}}{k} = \frac{1}{\alpha} \cdot \frac{\partial T}{\partial t} \quad (2)$$

$$\alpha = \frac{k}{\rho \cdot c_p} \quad (3)$$

where T is the temperature, x, y and z represent the Cartesian coordinate system, $\dot{q}$ is the rate of energy generation per unit volume, k is the thermal conductivity, t represents the time, ρ the mass density and c_p is the specific heat at constant pressure.

The finite-difference method was used to solve Equation (2). The temperature distribution inside the workpiece can thus be calculated based on a heat flux that enters through its surface. The heat flux depends on the erosion input parameters such as the burning voltage u_e and discharge current I_e as well as on the crater radius r_c, as shown in Equation (4). In Equation (4), F_c represents the erosion power factor, i.e. the amount of energy that flows into the anode. It was found in a previous study [13] that for the type of discharges used in this work a power factor of 0.35 can be considered, meaning that 35% of the whole discharge energy flows into the anode. The crater radius r_c in Equation (4) is described by the Equation (1) presented before.

$$q''(t) = F_c \cdot \frac{u_e(t) \cdot I_e(t)}{\pi \cdot r_c(t)^2} \quad (4)$$

Temperature distribution is thus calculated using three different types of nodal points, which define the whole workpiece: internal nodal points, adiabatic nodes (far away from the heat source, on the surfaces of the workpiece) and nodes in contact with the heat source. Solutions for these nodal points can be found in [14].

It is also important to mention that temperature-dependent material properties were considered in all the simulations, i.e. the thermal diffusivity presented in Equation (3) is not constant, but changes as a consequence of an increase on temperatures inside the workpiece. In addition, the latent heats of fusion and vaporization were also considered.

3.1. WEDM at high workpiece circumferential speeds

The aforementioned model approach was used to simulate the influence of the relative speed on erodes craters. Fig. 05 shows a comparison between simulated and measured craters regarding their top views, showing the similarities between its shapes, indicating a good qualitative correlation of results.

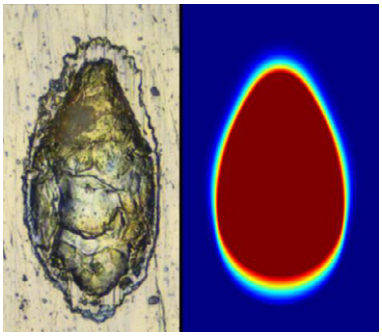

Fig. 05. Top views of single discharges (experiment vs. simulation)

To quantitatively show how the shape of eroded craters changes due to the relative speed between workpiece and wire electrode, the minor and major diameters of different craters were measured and compared to simulation results. Fig. 06 shows the results obtained by applying a discharge peak current of I_{peak} = 73 A, discharge duration of t_e = 1.25 µs and relative speeds between v_r = 0.5 m/s and 80 m/s. The major diameter represents the size of the crater in the direction of the relative speed while the minor diameter is the size of the crater perpendicularly to this direction (the maximal size in this direction). In this example, the major diameter is almost as large as twice the minor diameter when a relative speed of v_r = 80 m/s is applied. The simulated craters are stretched along the sliding direction of the heat source and show a small diameter reduction in perpendicular direction by increasing relative speeds. Experimental and simulation results do not fit completely, but errors are at most around 10%.

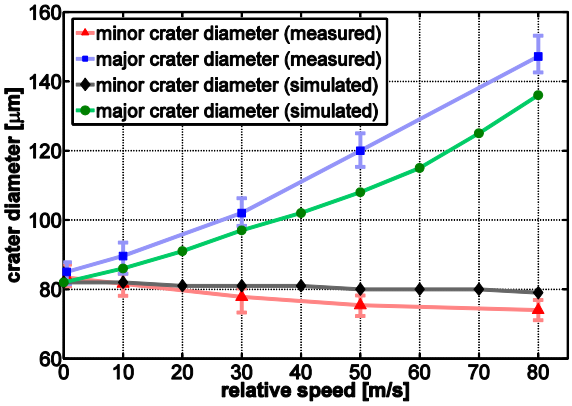

Fig. 06. Comparison between experimental and simulation results regarding the minor and major crater sizes as a function of relative speeds (I_{peak} = 73 A; t_e = 1.25 µs)

The influence of the relative speed on the volume of simulated craters is presented in Fig. 07. It can be seen that it increases as relative speed increases, being consistent with the results presented in Fig. 03, where the measured crater volume was found to increase by increasing relative speeds, although the curves show different trends. For a peak current of I_{peak} = 73 A and discharge duration of t_e = 1.25 µs, the simulated volume of eroded material per crater varies from approximately 12,000 µm^3 up to 17,000 µm^3 by rising the relative speed from v_r = 0.5 m/s to 80 m/s, while for I_{peak} = 157 A, it varies between around 33,000 µm^3 up to 43,000 µm^3 for the same of relative speeds up to 80 m/s.

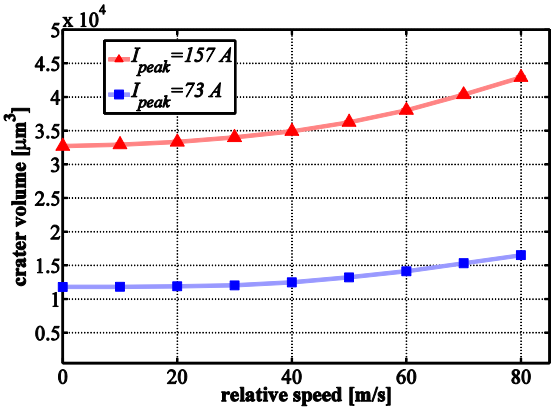

Fig. 07. Eroded volume per single discharge as a function of relative speeds (I_{peak} = 73 and 157 A; t_e = 1.25 and 1.35 µs)

Furthermore, the average nodal temperature, taking into consideration all nodes that reached temperatures higher than the melting temperature (T_{melt} = 1180 K), was calculated for different relative speeds and is presented in Fig. 08. It decreases by increasing the relative speed, indicating that higher melting efficiencies

are achieved when higher relative speeds are applied, i.e. for higher relative speeds the discharge energy is more efficiently used for melting more material rather than for overheating the melting pool. This is, thus, one of the reasons why higher material removal rates were achieved by increasing the relative speed between wire electrode and workpiece (Fig. 03).

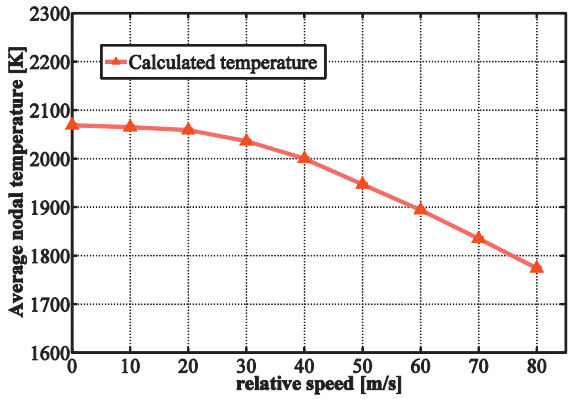

Fig. 08. Influence of relative speed on the average nodal temperature within the melting pool for brass (I_{peak} = 73 A; t_e = 1.25 µs)

4. High relative speeds during WEDD

High relative speeds can influence wire electrical discharge dressing to a great extension. The results presented so far are especially important when on-machine wire electrical discharge dressing of metal bonded diamond wheels is carried out. Dressing is considered a non-productive time, and for this reason has to be carried out as fast as possible inside the grinding machine. Thus, high material removal rates have to be achieved in order to maximize grinding performance. The relative speed can thus help making the electrical discharge dressing feasible, since material removal rates can be increased as relative speeds are increased. By dressing a bronze-based metal bonded diamond wheel with diamonds of equivalent diameters of 46 µm, material removal rates up to 100 mm^3/min were achieved. This represents a removal rate as high as about 10 times what can be achieved when conventional dressing method is used, i.e. when metal bonded diamond wheels are conditioned by SiC-wheels.

The relative speed also helps preventing arcing during EDD, which can occur near to the diamonds and cause thermal damages to these abrasives. Arcing can take place at the border between the diamond and the metal bond, since at these locations there is a concentration of electric field [15, 16]. The relative speed prevents consecutive discharges to occur at the same locations and thus arcing is not possible to occur, helping to protect the diamonds.

The relative speed can help reduce the possibilities of thermal damages to the diamonds. The same model approach presented before was used to predict diamond graphitization, in which a diamond embedded in bronze was assumed and a time time-dependent heat source was applied in the center point of the diamond. First a static heat source was considered and finally a moving heat source was applied. Fig 09 illustrates a schematic representation of the assumptions made to simulate diamond graphitization. The activation energy required to transform diamond into graphite was modeled similarly as for a latent heat, in other words, after reaching the graphitization temperature, the activation energy has first to be overcome before graphite is formed. An activation energy 728 KJ/mol [17] was used as input for the model, while the graphitization temperature was considered to be T_{graph} = 1,800 K (graphitization in the absence of oxygen). Diamond has a high thermal conductivity (k = 2,000 W/mK was assumed [18]), a specific heat at constant pressure of c_p = 509 J/kgK and mass density of 3500 Kg/m^3.

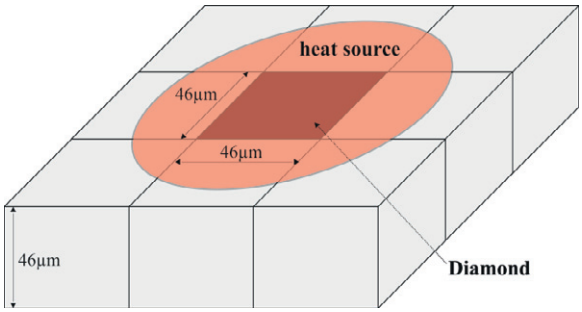

Fig. 09. Schematic representation of heat source applied to a diamond of equivalent diameter of 46 µm embedded in bronze bond material

Fig. 10 shows the amount of nodes that reached enough energy for graphitization consideration two different diamond sizes, namely D26 and D46, modeled as cubes. The cubes were spatially discretized with an equal distance of 1 µm between consecutive nodes (Δx = Δy = Δz), resulting in a total of 17,576 and 97,336 nodes, respectively in cubes of length 26 and 46 µm. Pulse discharges types *I1* to *I6* were applied in these simulations (Table 1) and a power factor F_c = 0.35 was assumed. For a D46 diamond, one can see that graphitization occurs only for more energetic erosion pulses (*I5* and *I6*). More graphitization is expected for smaller diamond sizes as shown in Fig. 10. In this case, thermal heat can stay more concentrated in the diamond since it has a smaller volume in comparison with a D46 diamond, where the heat can dissipate faster.

Finally, another model approach was tested in which a moving heat source was considered, i.e. the heat source was assumed to start near to the diamond and slip over it. All six different pulses used before were considered

and a relative speed of 80 m/s was used. For diamonds D46, graphitization was not obtained for all types of discharges, while for a D26 diamonds, only in the case of using the *I6* discharge pulse, 8 nodes out of a total of 17,576 reached enough energy for graphitization. This approach is closer to reality and indicates that even using high discharge energies, little or no thermal damages are expected to the diamonds during EDD, and that high relative speeds help minimizing the possibilities of thermal damages to the diamonds.

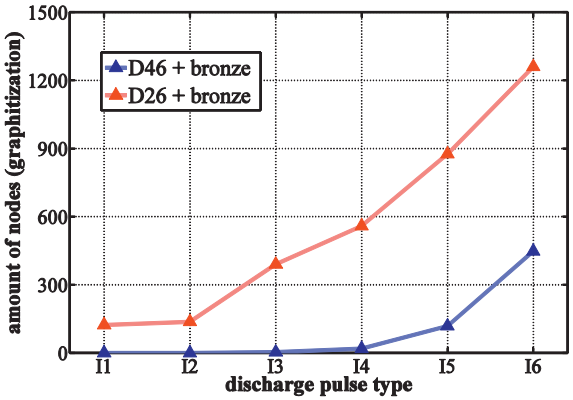

Fig. 10. Simulation of diamond graphitization due to single EDM discharges in diamonds of equivalent diameters of 26 and 46 μm

5. Conclusions

Wire electrical discharge dressing uses relative speeds that are typically not found in other EDM applications. Dressing is usually performed at grinding speeds, so that erosion can take place at speeds around 100 m/s. It was found that for the types of erosion pulses used in this work, the plasma channel easily slides over the anode, creating elongated craters. Not only the size of the craters is influenced by the relative speeds but also the material removal per single discharge is considerably affected. The material removal was found to increase as relative speeds are increased. Based on simulation results using a thermo-electrical model to describe the EDM process, it was found that higher melting efficiencies can be achieved when higher relative speeds are applied. In this case, the energy available in a single discharge can be better used to warm up and melt more material rather than to overheat the melting pool, and thus more material can be removed by a single discharge as the relative speed is increased.

Regarding electrical discharge dressing, it can be stated that the relative speed is an important variable for the process. It helps to increase material removal rates and consequently to reduce non-productive time, to avoid arcing occurring near to the diamonds, since consecutive discharges cannot occur in the same location, and to reduce the probability of diamond graphitization, since the discharge energy cannot concentrate on these abrasives. In other words, high relative speeds are strongly recommended in electrical discharge dressing, helping to make this process feasible for on-machine conditioning metal bonded diamond wheels.

References

[1] Yahagi, Y., Koyano, T., Kunieda, M., Yang, X., 2012. Micro Drilling EDM with High Rotation Speed of Tool Electrode Using the Electrostatic Induction Feeding Method, Procedia CIRP 1, p. 162.
[2] Haddad, M.J., Fadaei Tehrani, A., 2008. Material removal rate (MRR) study in the cylindrical wire electrical discharge turning (CWEDT) process, Journal of Materials Processing Technology 199(1-3), p. 369.
[3] Haddad, M.J., Tehrani, A.F., 2008. Investigation of cylindrical wire electrical discharge turning (CWEDT) of AISI D3 tool steel based on statistical analysis, Journal of Materials Processing Technology 198(1-3), p. 77.
[4] Mohammadi, A., Tehrani, A.F., Emanian, E., Karimi, D., 2008. Statistical analysis of wire electrical discharge turning on material removal rate, Journal of Materials Processing Technology 205(1-3), p. 283.
[5] Masuzawa, T., Fujino, M., Kobayashi, K., Suzuki, T., Kinoshita, N., 1985. Wire Electro-Discharge Grinding for Micro-Machining, Annals of CIRP 34(1), p. 431.
[6] Masuzawa, T., Yamaguchi, M., Fujino, M., 2005. Surface finishing of micropins produced by WEDG, Annals of CIRP 54(1), p. 171.
[7] Weingartner, E., Jaumann, S., Kuster, F., Boccadoro, M., 2010. Special wire guide for on-machine wire electrical discharge dressing of metal bonded grinding wheels, Annals of CIRP 59(1), p. 227.
[8] Weingartner, E., Jaumann, S., Kuster, F., Wegener, K., 2010. On-machine wire electrical discharge dressing (WEDD) of metal-bonded grinding wheels, International Journal of Advanced Manufacturing Technology 49(9-12), p. 1001.
[9] Wang, X.K., Ying, B.G., Liu, W.G., 1996. EDM dressing of fine grain super abrasive grinding wheel, Journal of Materials Processing Technology 62(4), p. 299.
[10] Matoorian, P., Sulaiman, S., Ahmad, M.M.H.M., 2008. An experimental study for optimization of electrical discharge turning (EDT) process, Journal of Materials Processing Technology 204(1-3), p. 350.
[11] Kunieda, M., Kameyama, A., 2010. Study on decreasing tool wear in EDM due to arc spots sliding on electrodes, Precision Engineering 34(3), p. 546.
[12] Uhlmann, E., Piltz, S., Jerzembeck, S., 2005. Micro-machining of cylindrical parts by electrical discharge grinding, Journal of Materials Processing Technology 160(1), p. 15.
[13] Weingärtner, E., Roth, R., Kuster, F., Boccadoro, M., Fiebelkorn, F., 2012. Electrical discharge dressing and its influence on metal bonded diamond wheels, CIRP Annals - Manufacturing Technology 61(1), p. 183.
[14] Incropera, F., DeWitt, D., Bergman, T., Lavine, A., 2006. Fundamentals of Heat and Mass Transfer, 6th Edition, Wiley.
[15] Klink, A., 2010. Wire electro discharge trueing and dressing of fine grinding wheels, Annals of CIRP 59(1), p. 235.
[16] Chen, H., Li, J.C.M., 2000. Anodic metal matrix removal rate in electrolytic in-process dressing I: Two-dimensional modeling, Journal of Applied Physics 87(6), p. 3151.
[17] Davies, G., Evans, T., 1972. Graphitization of Diamond at Zero Pressure and at a High Pressure, Proceedings of the Royal Society of London Series A, Mathematical and Physical Sciences, 328, p. 413.
[18] Field, J.E., 1979. The Properties of diamond: Academic Press, London.